Iron-doped nickel phosphide hollow nanospheres synthesized by solvothermal phosphidization of layered double hydroxides for electrocatalytic oxygen evolution

Shuling Liu* Zeyi Wang, Jinyu Du, Yichuang Xing, Yanling Hu, Yujie Ma, Xinyi Lu Chao Wang*

Department of Chemistry and Chemical Engineering, The Youth Innovation Team of Shaanxi Universities, Shaanxi University of Science and Technology, Xi'an, Shaanxi 710021, China

* Corresponding author:
E-mail address: shulingliu@aliyun.com
cwang@sust.edu.cn

1. Experimental

Chemicals

Nickel (II) nitrate hexahydrate ($Ni(NO_3)_2 \cdot 6H_2O$; Guanghua Chemical Reagent;

AR 98.0%), potassium hydroxide (KOH; Kermel Chemical Reagent; AR 85.0%), white phosphorous (P_4; Fuchen Chemical Reagent; AR), ethanol (C_2H_5OH;Rionlon Chemical Reagent; AR 99.7%), N, n-dimethylformamide (C_3H_7NO; Fuyu chemical ; reagent AR 99.5%)) benzene (C_6H_6; Hushi Chemical Reagent; AR 99.5%),methanol (CH_3OH; Guanghua Chemical Reagent; AR 99.5%), hydrochloric acid (HCl; Kelong Chemical Reagent; AR 38%),ferrous sulfate heptahydrate ($FeSO_4·7H_2O$; Tianli Chemical Reagent; AR 99.0%), Ammonium fluoride (NH_4F; Oberkai chemical reagent; AR 99.0%),sodium sulfate anhydrous (Na_2SO_4; Damao Chemical Reagent; AR 99.0%), potassium nitrate (KNO_3; Hengxing Chemical Reagent; AR 99.0%), urea (H_2NCONH_2 Damao Chemical Reagent; AR 99.0%), tetramethylammonium hydroxide pentahydrate ($C_4H_{13}NO·5H_2O$; Macklin Chemical Reagent; AR 97.0%), Ni foam (thickness 1.0mm) were used as received unless stated otherwise. Doubly distilled water was used throughout the experiment.

Prior to experiments, NF (3×2 cm^2) were ultrasonically cleaned in hydrochloric acid (0.1 M), acetone and ethanol consecutively for 10 min each to remove contaminants and surface oxides, then rinsed with deionized water, dried in oven and stored for subsequent use.

Preparation of $Ni(OH)_2$/NF

$Ni(NO_3)_2·6H_2O$ (2 mmol), NH_4F (8 mmol) and urea (20 mmol) were mixed in 30 mL of water. The resulting solution was poured into a 50 ml Teflon-lined autoclave with a piece of 3 × 2 cm^{-2} cleaned NF. The hydrothermal process was carried out at 120 ℃ in an electric oven for 6 h. After natural cooling to room temperature, the $Ni(OH)_2$

coated on NF was washed with deionized water, then blown dry under a stream of compressed air. The mass of $Ni(OH)_2$ on NF is weighed by a laboratory balance to 5.5 mg cm^{-2}.

Preparation of Ni_2P/NF

The 30 ml DMF (N, N-dimethylformamide) were added to 50 ml Teflon-lined autoclave, and the prepared $Ni(OH)_2$/NF was into the Teflon-lined autoclave leaning against the wall, with 0.6 mmol white phosphorus (P_4) added. The autoclave was kept at 180℃ for 2 h. After natural cooling, the Ni_2P/NF was removed from the autoclave, washed with benzene, ethanol and water, and dried under vacuum at 60 ℃ for 6 h. The mass of Ni_2P/NF on NF is weighed by a laboratory balance to 3.0 mg cm^{-2}.

2. Instrumentation

X-ray photoelectron spectroscopy (XPS) was carried out using a Kratos Axis Supra spectrometer at room temperature and ultra-high vacuum (UHV) conditions. The instrument was equipped with monochromatic Al Kα source 1486.6 eV (15 mA, 15 kV), and hemispherical analyser with hybrid magnetic and electrostatic lens for enhanced electron collection. Survey and detailed XPS spectra were acquired at normal emission with the fixed pass energy of 160 eV and 40 eV, respectively. All spectra were charge-corrected to the hydrocarbon peak set to 284.6 eV. The Kratos charge neutralizer system was used on all specimens. Data analysis was based on a standard deconvolution method using mixed Gaussian (G) and Lorentzian (L) line shape (G = 70% and L = 30%, Gaussian - Lorentzian product) for each component. Spectra were analyzed using CasaXPS software (version 2.3.16). X-ray diffraction (XRD) was

acquired using (D8 ADVANCE, Bruker) diffractometer having Cu Kα (λ=1.54 A) source. The instrument was operated at 30 mA current voltage and 40 kV. Field emission scanning electron microscope (S-4800, Hitachi, Japan) and transmission electron microscope (FEI-Tecnai G2 F20) were used to observe the morphology of the catalyst. A concentric nebulizer was used with a cyclonic spray chamber.

Electrochemical measurements were carried out using electrochemical workstations (CHI660E and ParSTAT MC). The geometric area of the working electrode immersed in the electrolyte is controlled to 1 cm^2. The Tafel slope (b) is calculated by Eq. 1.

$$\eta = b \log j \quad (1)$$

where η is the overpotential, b is the Tafel slope, and j is the current density. AC electrochemical impedance spectroscopy (EIS) is performed with the alternating voltage amplitude at 5 mV in the range of 100 kHz to 1 Hz. The solution resistance acquired from the EIS is used for iR compensation, and all the linear sweep voltammetry and galvanostatic measurements are iR compensated. The potentials are reported in reversible hydrogen electrode (RHE) scale unless otherwise stated.

3. X-ray photoelectron spectroscop

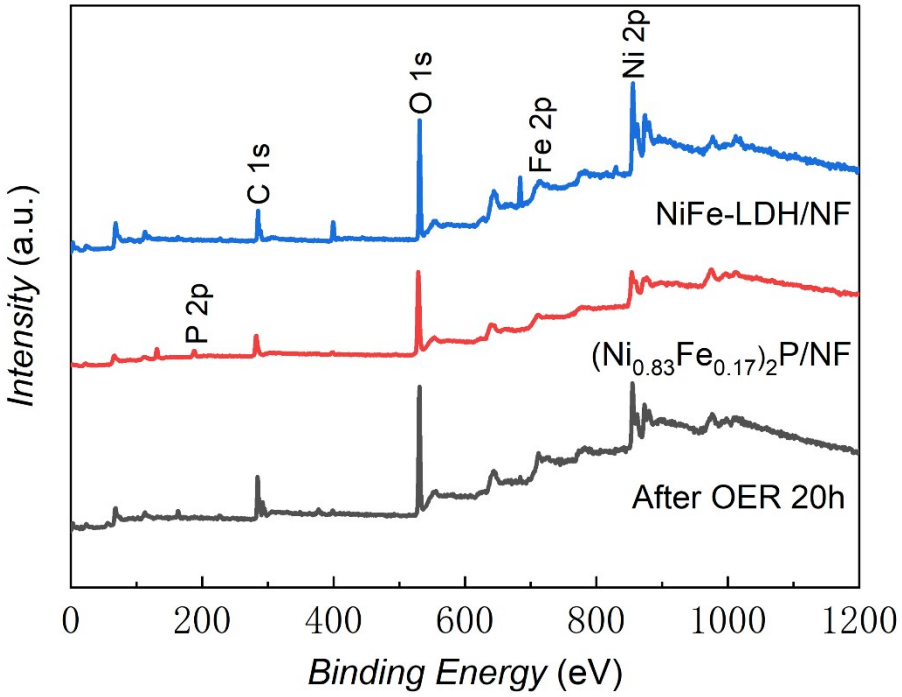

Figure S1. (a) Observed XPS spectra of NiFe-LDH/NF and $(Ni_{0.83}Fe_{0.17})_2P$/NF and $(Ni_{0.83}Fe_{0.17})_2P$/NF after 20h OER testing;

4. Electrochemistry

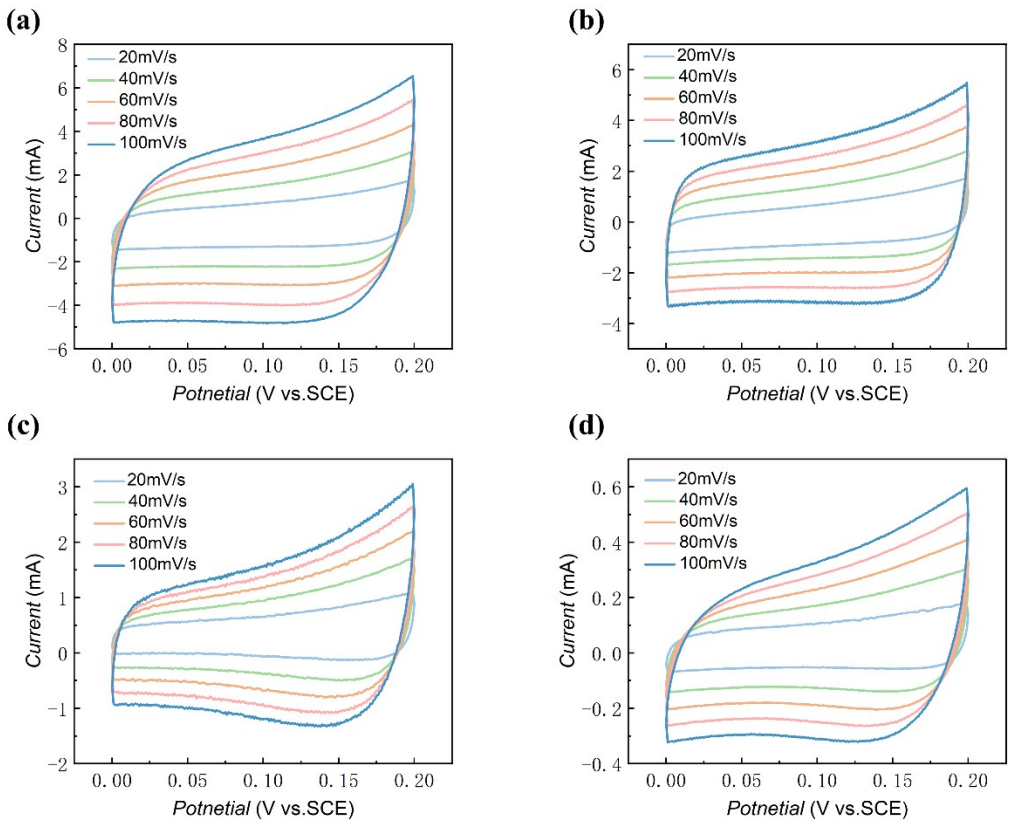

Figure S2. (a-d) CV of Ni_2P/NF, $(Ni_{0.83}Fe_{0.17})_2P$/NF, NiFe-LDH/NF and NF at different scan rates (20, 40, 60, 80, and 100 mV s^{-1}) in 0-0.2 V in 1 M KOH.

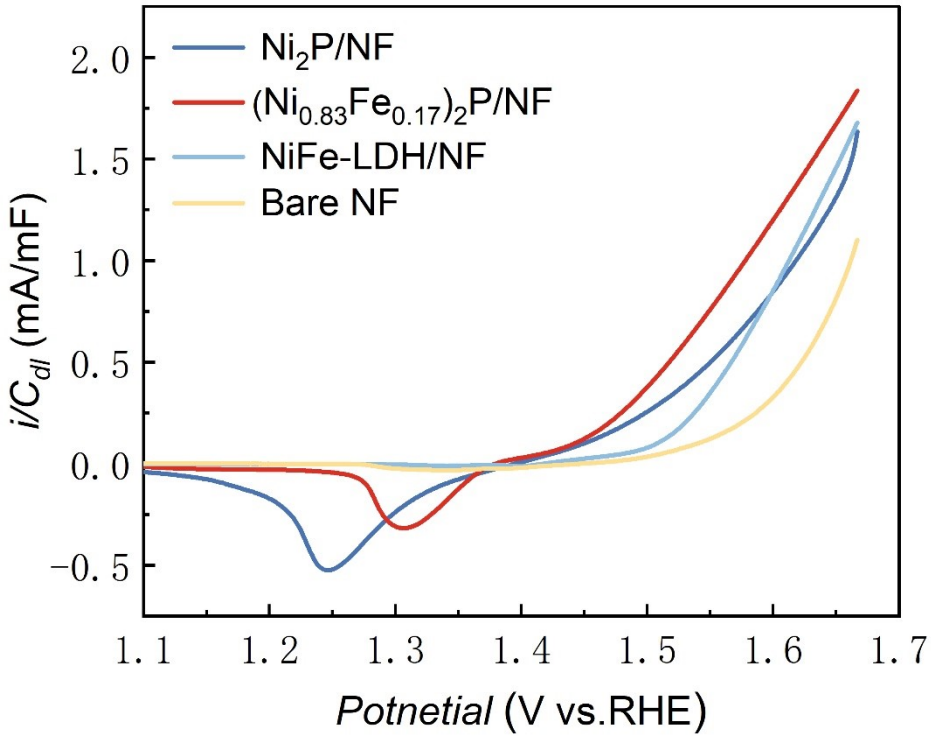

Figure S3. Plots of the OER current densities normalized to C_{dl}.

For methanol electrooxidation in alkaline solution,

$CH_3OH + 6\ OH^- \rightarrow CO_2 + 5\ H_2O + 6\ e^-$

the standard redox potential (E^o) is 0.02 V_{RHE}. Assuming that the current-potential behavior follows the Butler-Vomer kinetics, and that at high overpotential, the cathodic current density is negligible, the current-potential relationship is described by Eq. 2,3,

$$j = j_0 e^{\beta f \eta} \quad (2)$$

$$f = F / RT \quad (3)$$

where j is the current density, j_0 is the exchange current density, β is the transfer. Where j is the current density, j_0 is the exchange current density, β is the transfer coefficient, η is the overpotential, and other variables have their standard meanings. By taking logarithm of Eq. 4, there is

$$\log j = \log j_0 + \alpha f \eta / 2.303RT \quad (4)$$

Therefore, by plotting the $\log j$ vs. η plot, the j_0 can be acquired from the intercept. The j_0 of MOR for Ni_2P, $(Ni_{0.83}Fe_{0.17})_2P$/NF are 5.49×10^{-14} mA cm^{-2} and 3.98×10^{-16} mA cm^{-2}, respectively. These values are significantly smaller than the Pt based electrocatalysts for MOR.[1, 2]

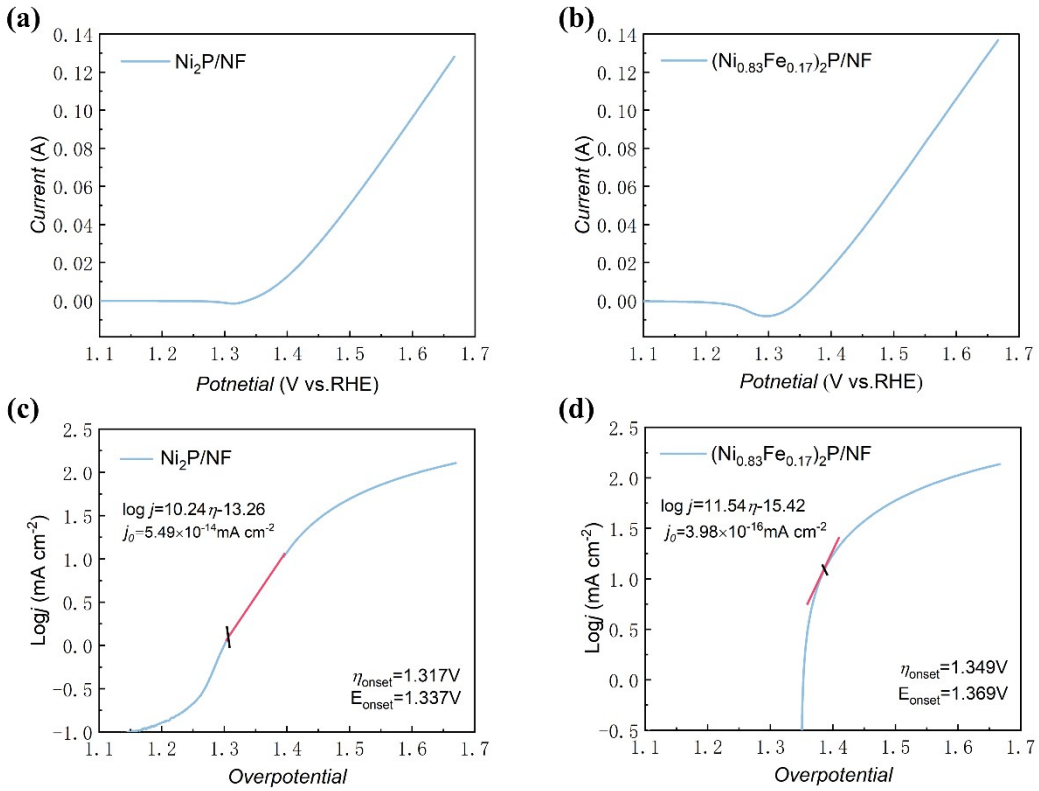

Figure S4. The LSV of the Ni_2P/NF and $(Ni_{0.83}Fe_{0.17})_2P$/NF electrodes in 0.5 M CH_3OH + 1 M KOH (scan rate 5 mV s^{-1})

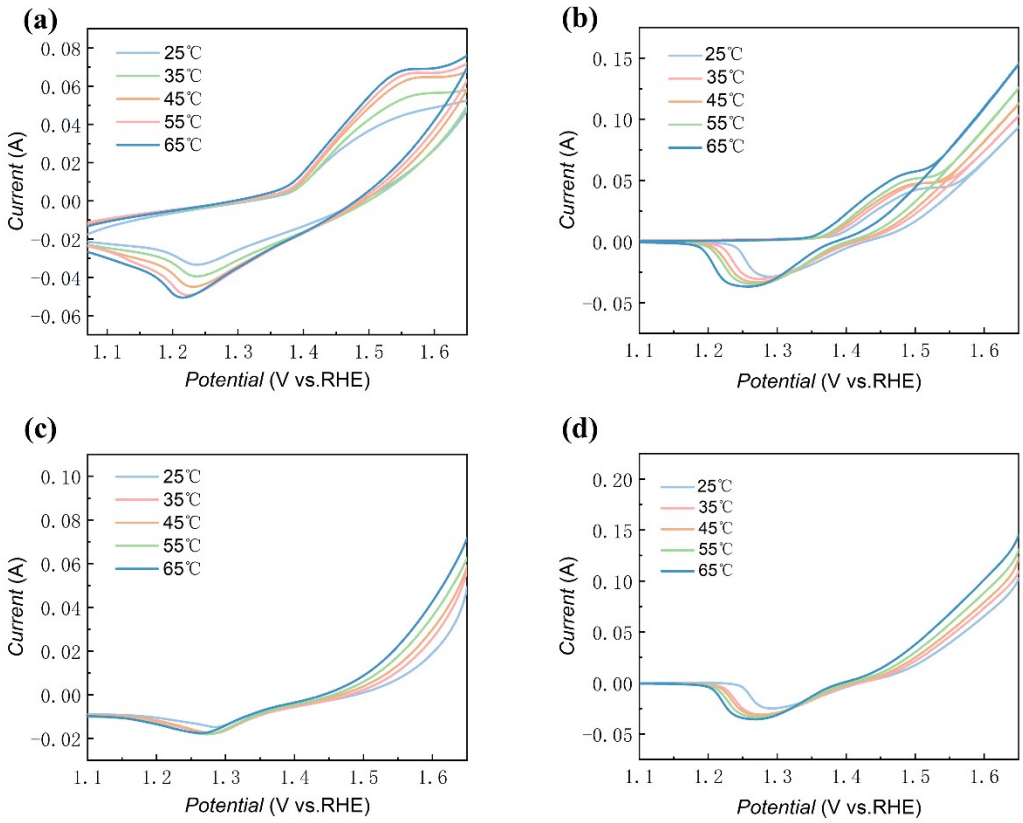

Figure S5. The CV and LSV of the (a, c) Ni_2P/NF and (b, d) $(Ni_{0.83}Fe_{0.17})_2P$/NF at different temperatures in 1 M KOH at scan rate 5 mV s^{-1}.

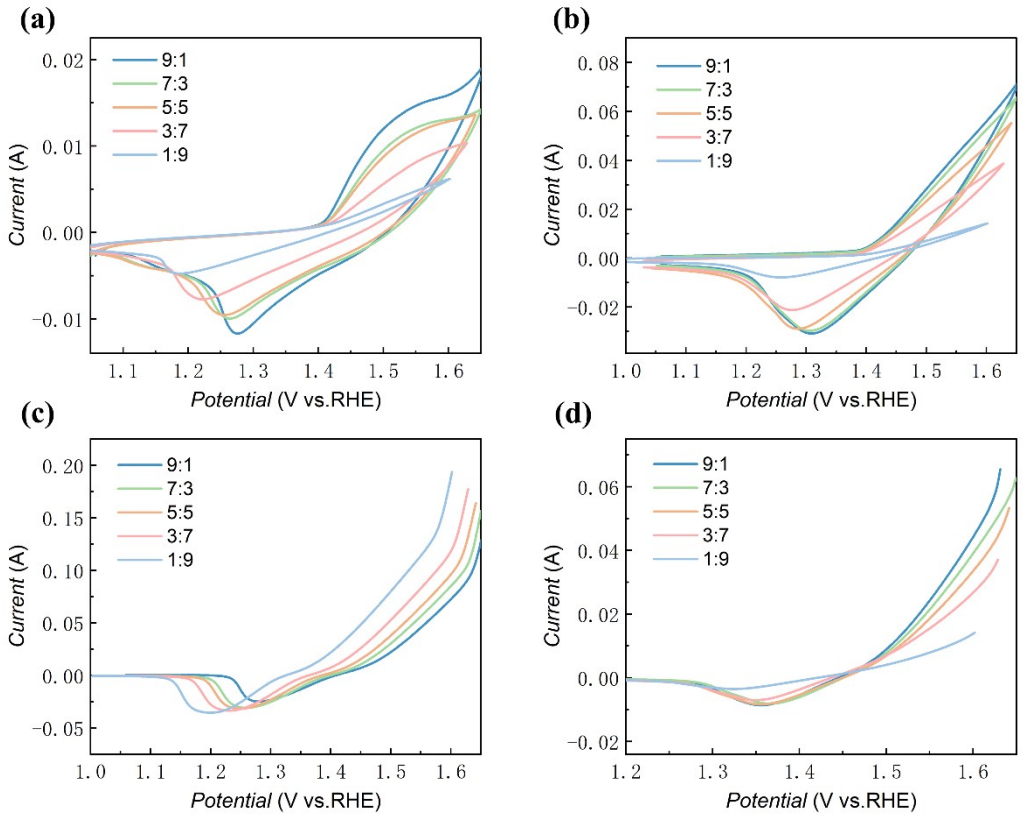

Figure S6. The CV and LSV of the (a, c) Ni_2P/NF and (b, d) $(Ni_{0.83}Fe_{0.17})_2P$/NF in different pH solutions (x M KOH + (1-x) M KNO_3, pH=13.84, 13.72, 13.57, 13.35, and 12.9) at scan rate 5 mV s^{-1}.

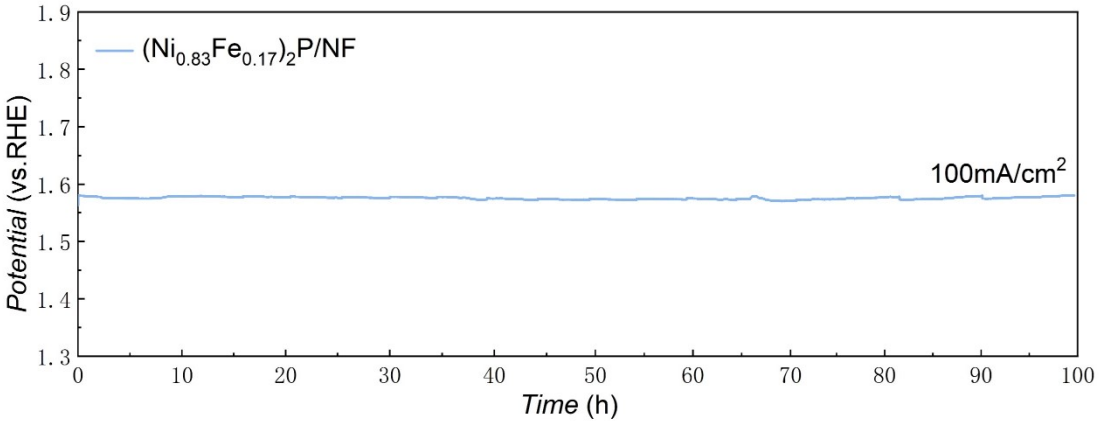

Figure S7. The time potential curve of the catalyst $(Ni_{0.83}Fe_{0.17})_2P$/NF with a constant current density of 100mA cm^{-2} was obtained at 1M KOH for about 100 h.

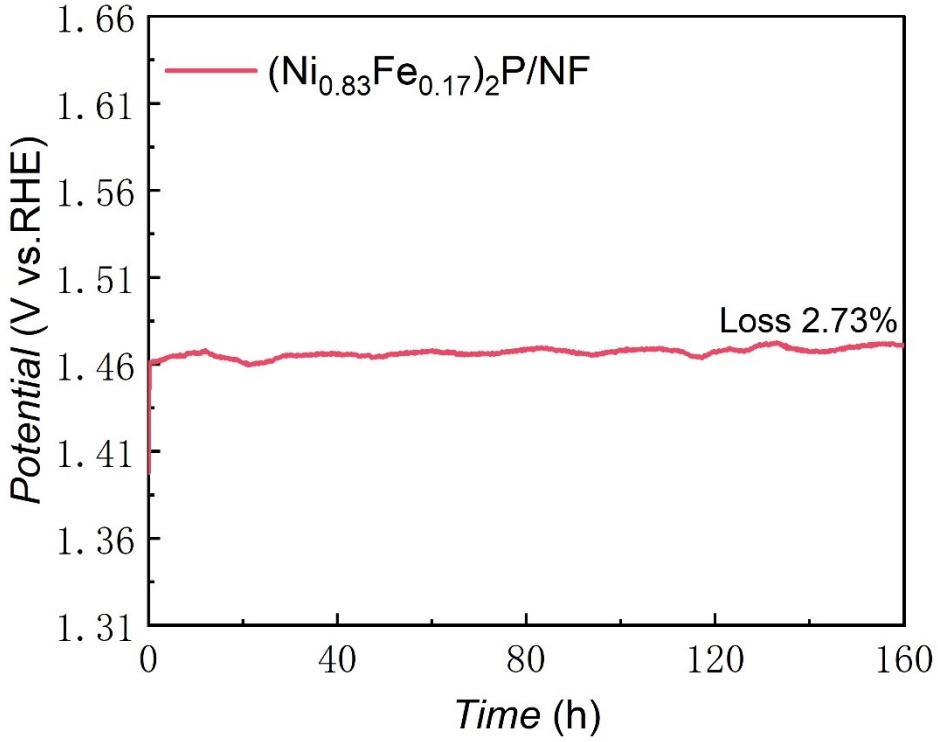

Figure S8. The time potential curve of the catalyst $(Ni_{0.83}Fe_{0.17})_2P$/NF with a constant current density of 10mA cm^{-2} was obtained at 1M KOH for about 160 h.

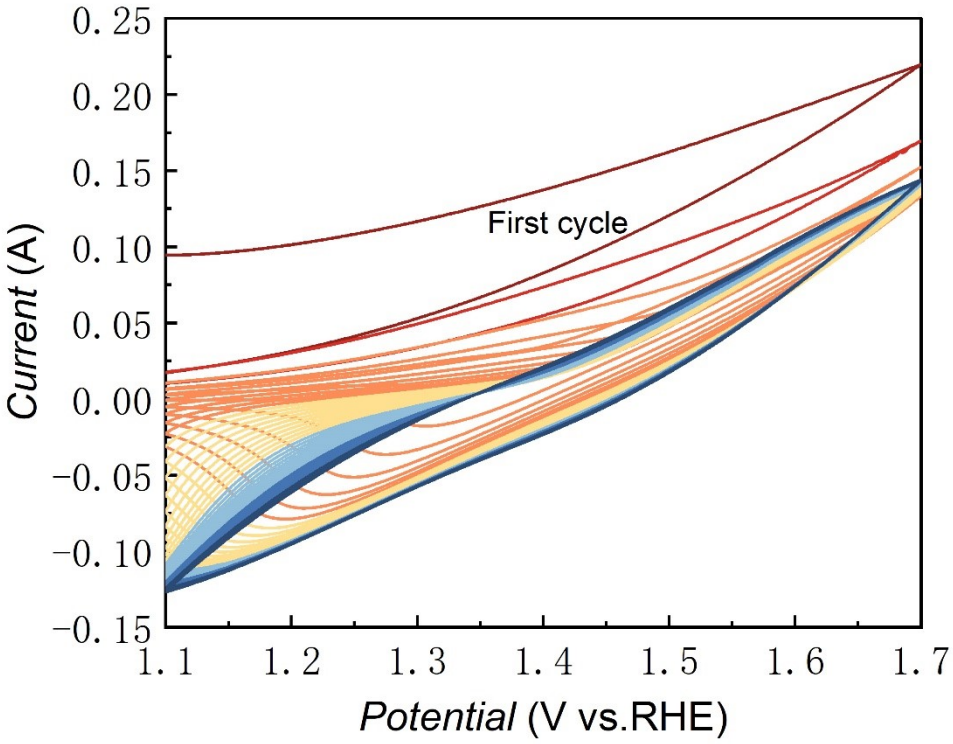

Figure S9. The first 50 CV cycles of $(Ni_{0.83}Fe_{0.17})_2P$/NF at 50 mV s^{-1} in 1M KOH.

5. EDS

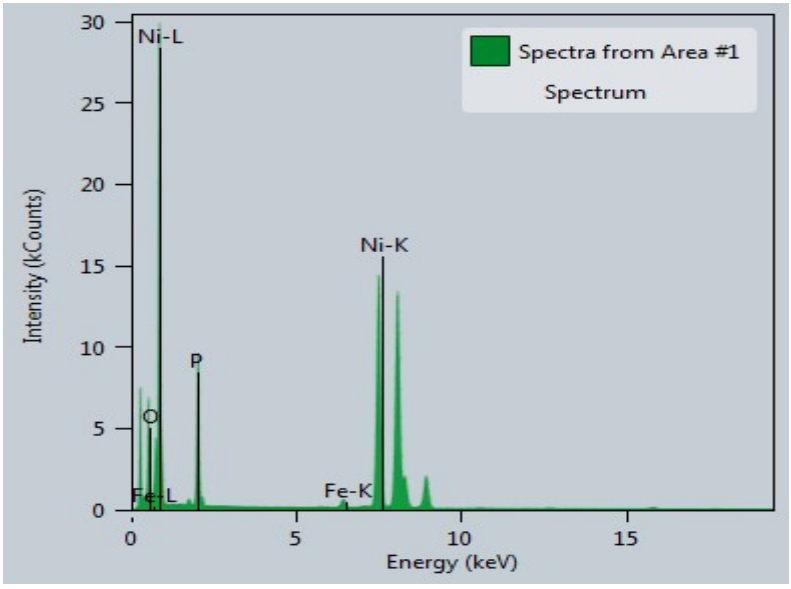

Figure S10. EDS spectrum obtained for $(Ni_{0.83}Fe_{0.17})_2P$ on Ni foam.

Table S1. Contents of the deposited films

		Atomic Percentage (%)		
		Ni	Fe	P
NiFe-LDH	XPS	90.72	9.28	-
	EDS	-	-	-
$(Ni_{0.83}Fe_{0.17})_2P$/NF	XPS	58.62	11.92	29.44
	EDS	64.62	1.93	33.45
Post 20h OER	XPS	91.84	8.16	-
	EDS	-	-	-

Table S2. EIS fitting results

	R_s / Ω	Error / %	R_{ct} / Ω	Error / %
Ni_2P/NF	2.86	0.21163	2.078	0.96
NiFe-LDH/NF	2.827	0.4443	2.256	1.43
$(Ni_{0.83}Fe_{0.17})_2P$/NF	1.281	0.25438	0.3293	1.86
Bare NF	25.26	1.3248	56.53	3.22

6. SEM

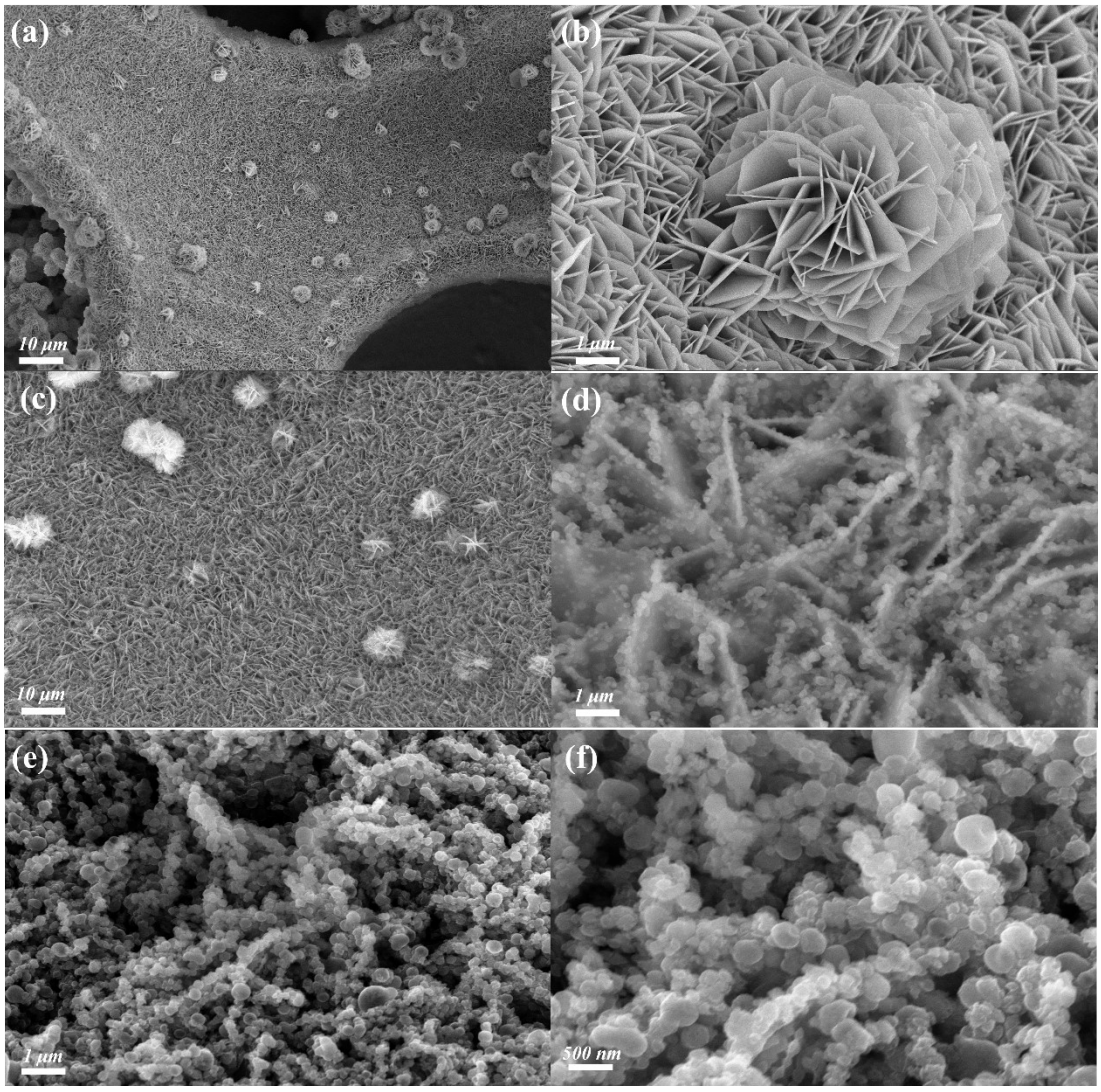

Figure S11. SEM images of (a-b) NiFe-LDH/NF, (c-d) $(Ni_{0.83}Fe_{0.17})_2P$/NF, (e-f) $(Ni_{0.83}Fe_{0.17})_2P$/NF after the long-term galvanostatic OER test.

6. TEM

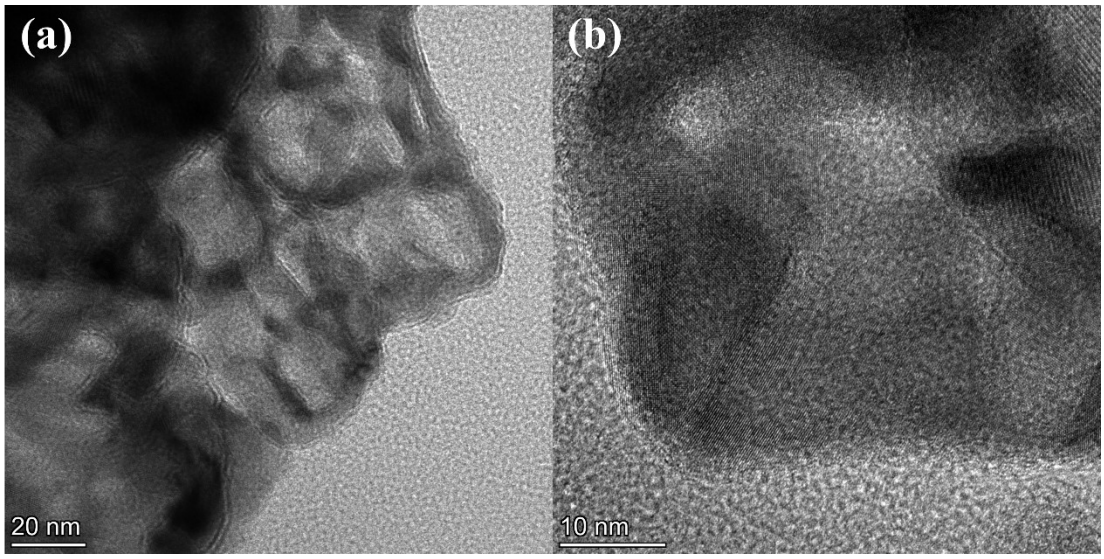

Figure S12. (a) TEM and (b) HRTEM images of $(Ni_{0.83}Fe_{0.17})_2P$/NF.

6. Activity comparison

Table S3. OER activity comparison in alkaline solutions

Catalysts	Loading/mg cm^{-2}	η at 10 mA cm^{-2}	Tafel slope/mV dec^{-1}	References
$(Ni_{0.83}Fe_{0.17})_2P$	3mg	215mV	31.84	This work
Fe-(NiP_2/Ni_2P)/CNT	4mg	254mV	46.1	[3]
NiFeP@NiP/NF	3mg	227mV	60.7	[4]
NiFeP	0.2mg	265 mV	40.9	[5]
NiP_2/FeP/CNT	4mg	261mV	44.0	[6]
$Ni_{0.85}Fe_{0.15}PS$/NF	4mg	251mV	34.0	[7]
NiFe-P NiFe-P	3mg	233mV	42.5	[8]
$NiFe(OH)_x/NiP_x$/NF	2mg	220 mV	35	[9]

References

1. L. Chen, X. Liang, D. Wang, Z. Yang, C.-T. He, W. Zhao, J. Pei and Y. Xue, *ACS Applied Materials & Interfaces*, 2022, **14**, 27814-27822.
2. Y. Tong, X. Yan, J. Liang and S. X. Dou, *Small*, 2021, **17**, 1904126.
3. Y. Liu, B. Wang, K. Srinivas, M. Wang, Z. Chen, Z. Su, D. Liu, Y. Li, S. Wang and Y. Chen, *International Journal of Hydrogen Energy*, 2022, **47**, 12903-12913.

4. F. Diao, W. Huang, G. Ctistis, H. Wackerbarth, Y. Yang, P. Si, J. Zhang, X. Xiao and C. Engelbrekt, *ACS Applied Materials & Interfaces*, 2021, **13**, 23702-23713.
5. T. Wang, X.-Z. Fu and S. Wang, *Green Energy & Environment*, 2022, **7**, 365-371.
6. Y. Liu, B. Wang, Y. Lu, Z. Su, Y. Li, Q. Wu, D. Yang, Y. Chen and S. Wang, *Journal of Materials Science*, 2021, **56**, 16000-16009.
7. W. Peng, J. Li, K. Shen, L. Zheng, H. Tang, Y. Gong, J. Zhou, N. Chen, S. Zhao and M. Chen, *Journal of Materials Chemistry A*, 2020, **8**, 23580-23589.
8. P. Li and H. C. Zeng, *Journal of Materials Chemistry A*, 2018, **6**, 2231-2238.
9. P. Wang, T. Yu, L. Hao and X. Liu, *Journal of Power Sources*, 2024, **589**, 233749.